

A Water-Stable 3D Eu(III)-Organic Framework as a Bi-Functional Ratiometric Luminescent Sensor for Fast, Sensitive and Selective Detection of ODZ and Hg²⁺ in Aqueous Media

Xiuting Gao¹, Nana Chen¹, Minglei Cao², Yang Shi¹ and Qingfu Zhang^{1*}

¹College of Chemistry and Chemical Engineering, Liaocheng University, Liaocheng, Shandong 252059, China

²Shandong Ruijie New Material Co.Ltd, Liaocheng, Shandong 252000, China

*Corresponding author. Email: zhangqingfu@lcu.edu.cn

Synthesis of the H₂L ligand. The synthesis of 4,4'-(naphthalene-1,4-dicarbonyl)bis(azanediyl)dibenzoic acid (*H*₂*L*) was achieved by using a modified version of a previously reported procedure.^[S1] The sample of 4-aminobenzoic acid (1.09 g, 7.95 mmol) is added to the toluene solution of 1,4-naphthalenedicarbonylchloride (1.04 g, 4.11 mmol), and the resulting solution was refluxed for 8 h. After cooling to room temperature, the precipitate was filtrated and washed with chloroform to give *H*₂*L* as a white powder. Yield: 82%. H-NMR (DMSO-*d*₆, ppm): δ 10.90 (s, 2H, -OH), 8.96 (s, 2H, -CONH-), 8.30 (2H, Ar-H), 8.17 (2H, Ar-H), 7.97 (2H, Ar-H), 7.95 (2H, Ar-H), 7.84 (2H, Ar-H), 7.66 (2H, Ar-H).

SUPPORTING INFORMATION

S Chinese Journal of
Structural Chemistry

n SUPPLEMENTARY FIGURES

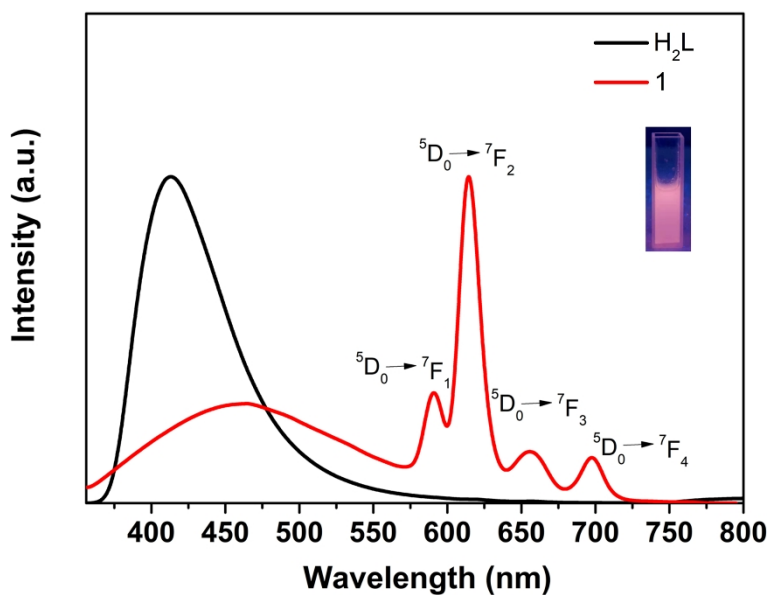


Figure S1. The emission spectra of H_2L ligand and **1** upon excitation at 326 nm. The inset shows the corresponding luminescence picture under UV-light irradiation of 254 nm.

SUPPORTING INFORMATION

S Chinese Journal of
Structural Chemistry

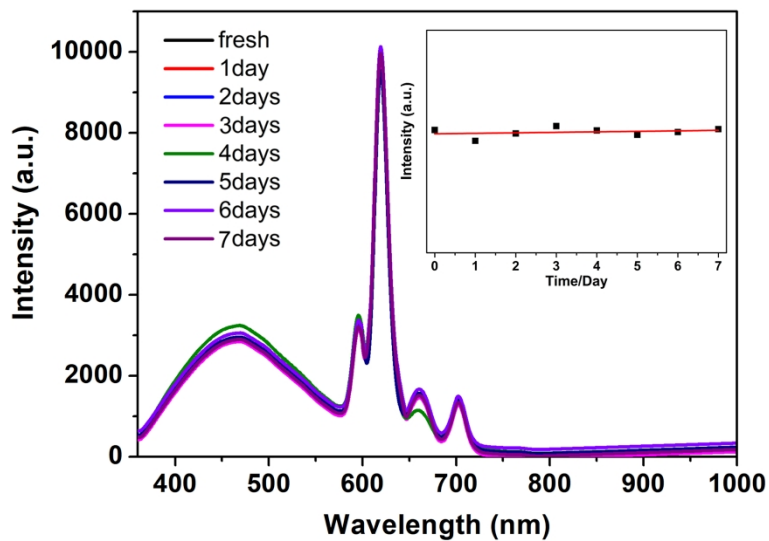


Figure S2. Day-to-day fluorescence stability of **1** in water.

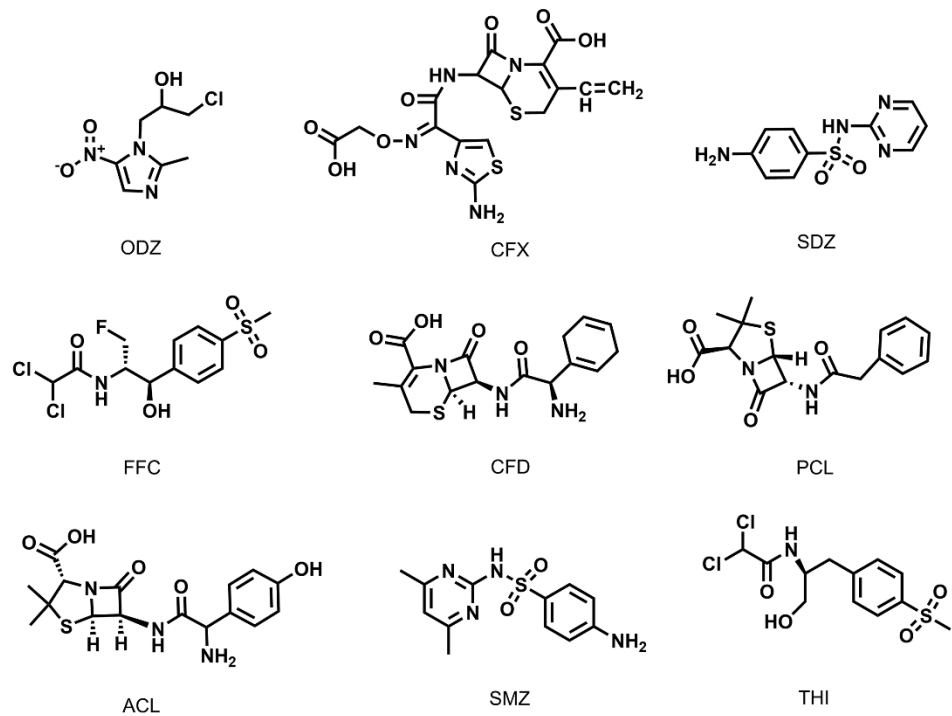


Figure S3. Molecular structures of the antibiotics.

SUPPORTING INFORMATION

S Chinese Journal of
Structural Chemistry

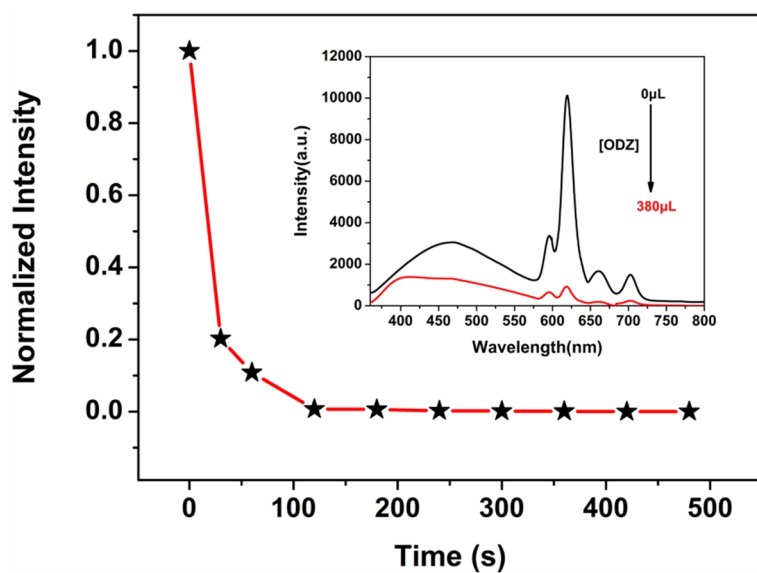


Figure S4. Luminescent response time of **1** toward ODZ (the inset shows the luminescence spectra of **1** before (0 s) and after (30 s) the addition of 380 μL of ODZ).

SUPPORTING INFORMATION

S Chinese Journal of
Structural Chemistry

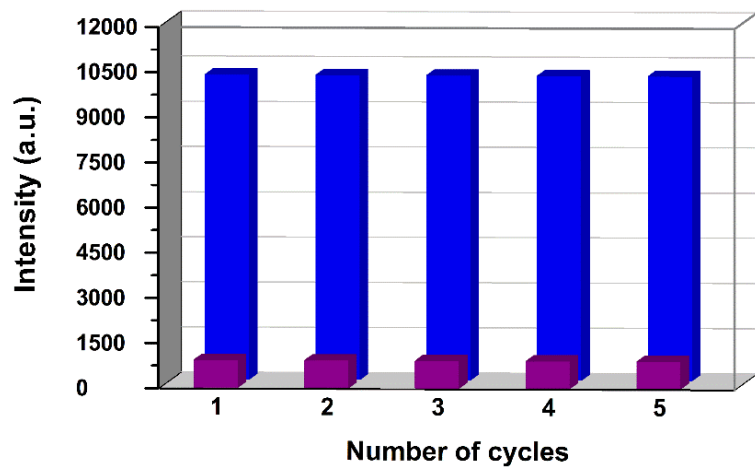


Figure S5. Recyclability experiments of **1** implemented with ODZ.

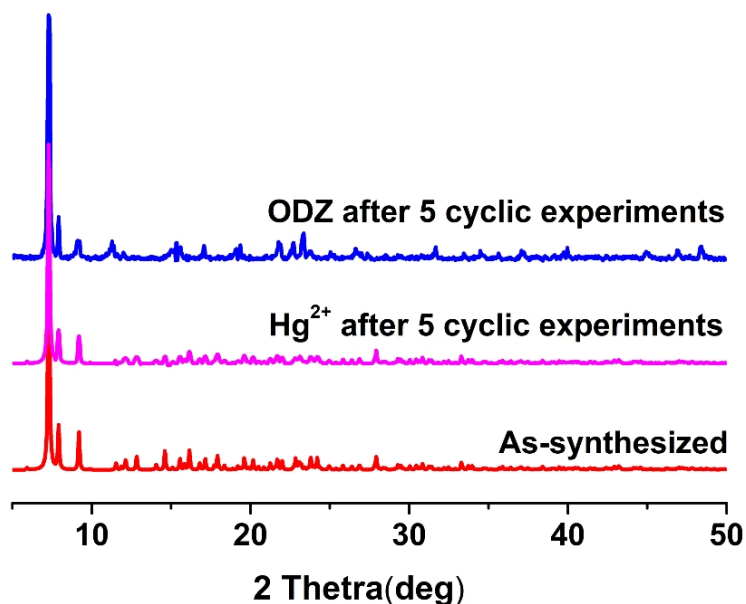


Figure S6. The PXRD patterns for **1** after 5 cyclic experiments.

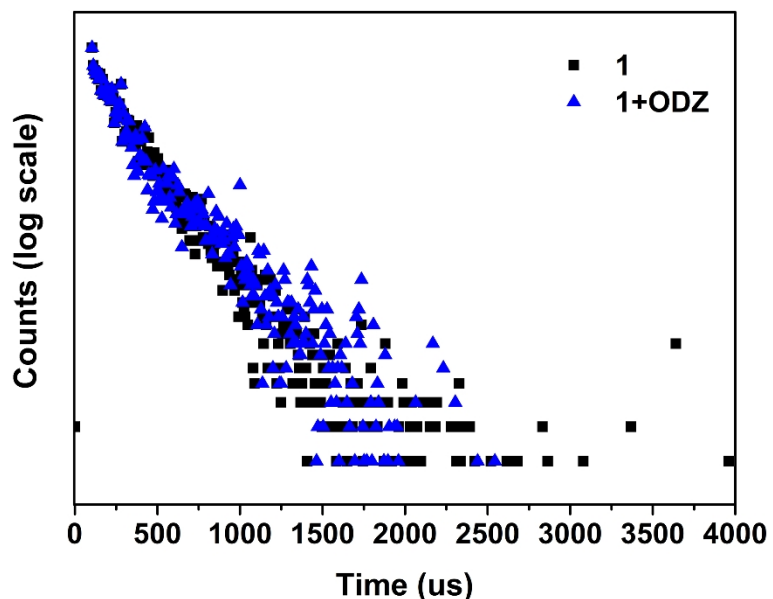


Figure S7. Time-resolved fluorescence decay of **1** in 619 nm before and after the addition of ODZ under excitation at 326 nm.

SUPPORTING INFORMATION

S Chinese Journal of
Structural Chemistry

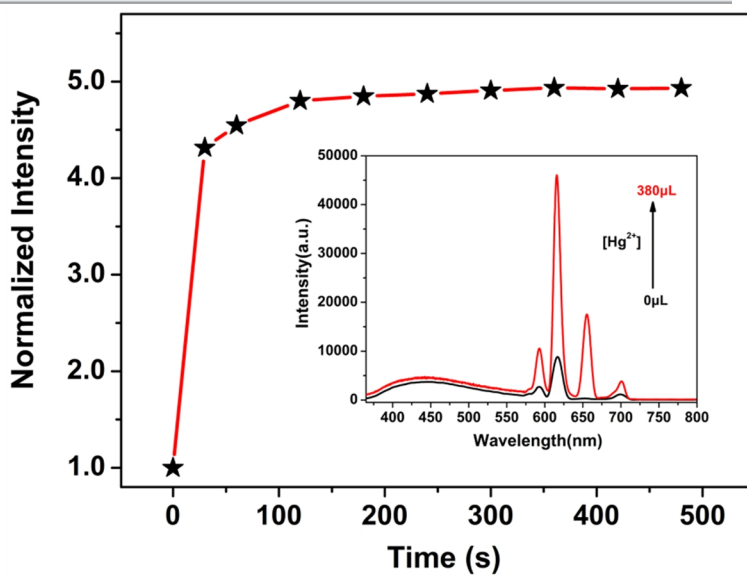


Figure S8. Luminescent response time of **1** toward Hg^{2+} (The inset shows the luminescence spectra of **1** before (0 s) and after (30 s) the addition of 380 μL of Hg^{2+}).

SUPPORTING INFORMATION

S Chinese Journal of
Structural Chemistry

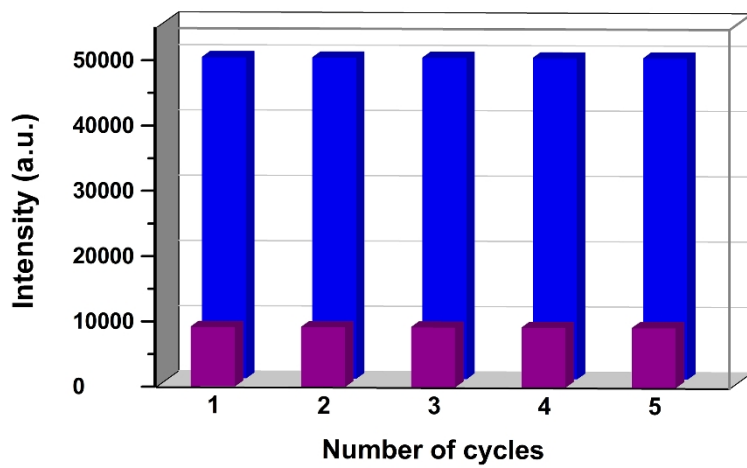


Figure S9. Recyclability experiments of **1** implemented with Hg^{2+} .

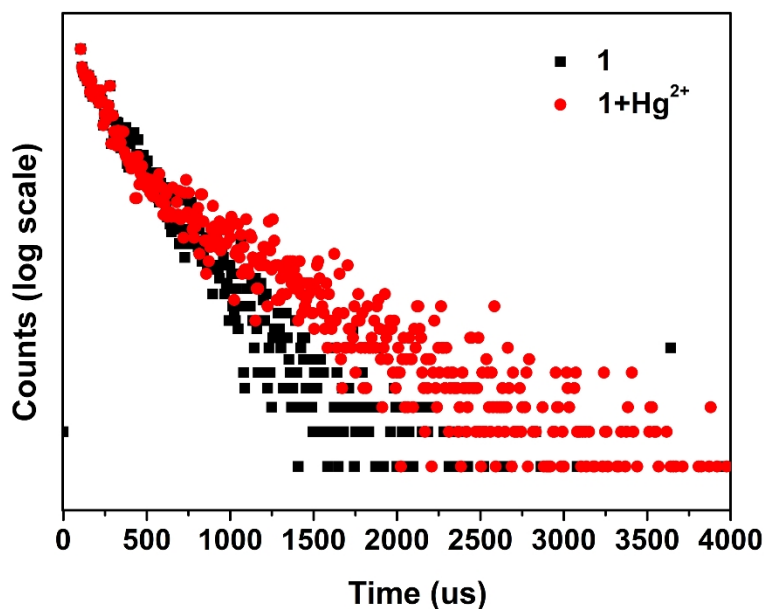


Figure S10. Time-resolved fluorescence decay of **1** in 619 nm before and after addition of Hg^{2+} under excitation at 326 nm.

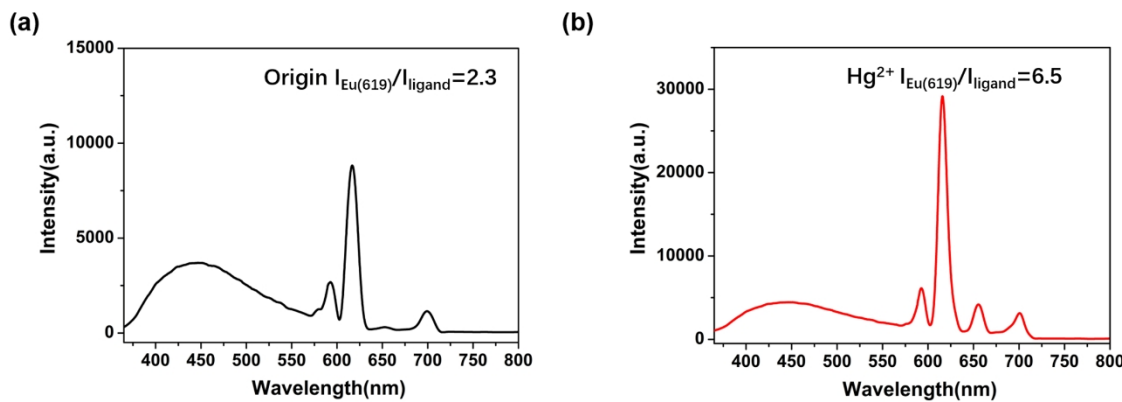


Figure S11. The emission spectra of **1** in the absence (black) and presence of Hg^{2+} (red) in aqueous solution upon excitation at 326 nm.

SUPPORTING INFORMATION

S Chinese Journal of
Structural Chemistry

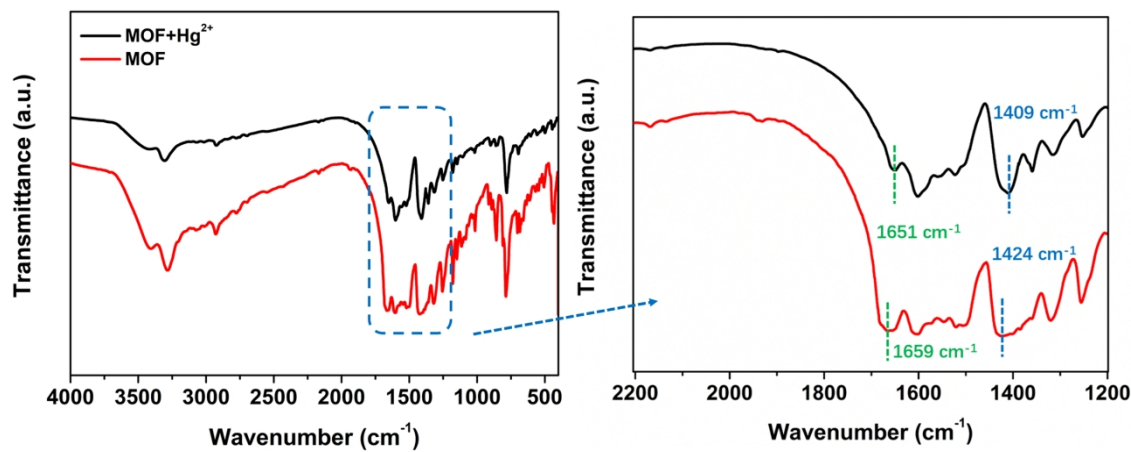


Figure S12. IR spectra of MOF and $\text{MOF}+\text{Hg}^{2+}$.

SUPPORTING INFORMATION

Table S1. Crystal Data and Structure Refinement Parameters for 1

Empirical formula	C ₅₂ H ₃₆ EuN ₄ O ₁₄
Formula weight	M _r = 1092.81
Crystal system	Orthorhombic
Space group	Pcc2
a (Å)	12.587(6)
b (Å)	44.67(2)
c (Å)	9.895(5)
V (Å ³)	5563(4)
Z	4
ρ _{calcd} (g·cm ⁻³)	1.305
μ (mm ⁻¹)	1.19
F(000)	2204
θ range (°)	2.66 to 28.051
Index ranges	-14≤h≤12, -48≤k≤53, -11≤l≤11
Data/restraints/parameters	9184/2161/567
GOF on F ²	1.093
R ₁ ^a , wR ₂ ^b [I > 2σ(I)]	0.0637, 0.1748

SUPPORTING INFORMATION

Table S2. Selected Bond Lengths (\AA) and Bond Angles ($^\circ$) for 1

Bond lengths			
Eu1-O4A	2.325(9)	Eu2-O6D	2.304(9)
Eu1-O4B	2.325(9)	Eu2-O6E	2.304(9)
Eu1-O3	2.353(9)	Eu2-O5	2.385(9)
Eu1-O3C	2.354(9)	Eu2-O5F	2.385(9)
Eu1-O13C	2.500(11)	Eu2-O14F	2.478(11)
Eu1-O13	2.500(11)	Eu2-O14	2.478(11)
Eu1-O9C	2.526(10)	Eu2-O11F	2.493(10)
Eu1-O9	2.526(10)	Eu2-O11	2.493(10)
Bond angles			
O4A-Eu1-O4B	94.4(4)	O6D-Eu2-O6E	92.9(4)
O4A-Eu1-O3	141.9(4)	O6D-Eu2-O5	87.5(3)
O4B-Eu1-O3	88.1(3)	O6E-Eu2-O5	141.8(4)
O4A-Eu1-O3C	88.1(3)	O6D-Eu2-O5F	141.8(4)
O4B-Eu1-O3C	141.9(4)	O6E-Eu2-O5F	87.5(3)
O3-Eu1-O3C	112.5(5)	O5-Eu2-O5F	114.9(5)
O4A-Eu1-O13C	147.0(3)	O6D-Eu2-O14F	79.8(3)
O4B-Eu1-O13C	78.9(3)	O6E-Eu2-O14F	148.3(4)
O3-Eu1-O13C	70.7(4)	O5-Eu2-O14F	69.2(4)
O3C-Eu1-O13C	78.6(3)	O5F-Eu2-O14F	80.1(3)
O4A-Eu1-O13	78.9(3)	O6D-Eu2-O14	148.3(4)
O4B-Eu1-O13	147.0(3)	O6E-Eu2-O14	79.8(3)
O3-Eu1-O13	78.6(3)	O5-Eu2-O14	80.1(3)
O3C-Eu1-O13	70.7(4)	O5F-Eu2-O14	69.2(4)
O13C-Eu1-O13	123.3(5)	O14F-Eu2-O14	121.4(5)
O4A-Eu1-O9C	75.2(3)	O6D-Eu2-O11F	71.1(3)
O4B-Eu1-O9C	73.4(3)	O6E-Eu2-O11F	76.5(3)
O3-Eu1-O9C	140.8(4)	O5-Eu2-O11F	138.3(3)
O3C-Eu1-O9C	70.6(3)	O5F-Eu2-O11F	71.9(3)
O13C-Eu1-O9C	71.9(3)	O14F-Eu2-O11F	72.0(3)
O13-Eu1-O9C	133.5(3)	O14-Eu2-O11F	134.8(3)
O4A-Eu1-O9	73.4(3)	O6D-Eu2-O11	76.5(3)
O4B-Eu1-O9	75.1(3)	O6E-Eu2-O11	71.1(3)
O3-Eu1-O9	70.6(3)	O5-Eu2-O11	71.9(3)
O3C-Eu1-O9	140.8(4)	O5F-Eu2-O11	138.3(3)
O13C-Eu1-O9	133.5(3)	O14F-Eu2-O11	134.8(3)
O13-Eu1-O9	71.9(3)	O14-Eu2-O11	72.0(3)
O9C-Eu1-O9	133.0(5)	O11F-Eu2-O11	132.2(4)

Symmetry codes: A: x, -y+1, z+1/2; B: -x+1, y, z+1/2; C: -x+1, -y+1, z; D: -x, y, z+1/2; E: x, -y, z+1/2; F: -x, -y, z

SUPPORTING INFORMATION

Table S3. Comparison of Detection Capacities of **1** toward ODZ with Other Reported MOF Materials

MOFs	Analyte	LOD (μM)	Ref.
[Cd ₃ (DBPT) ₂ (H ₂ O) ₄]·5H ₂ O	ODZ	5.0	S2
[Eu(cppa)(OH)]·xS	ODZ	0.52	S3
C ₂₃ H ₁₉ EuN ₄ O ₉ S ₂ ·0.5H ₂ O	ODZ	0.319	S4
[Tb(TATAB)(H ₂ O)]·2H ₂ O	ODZ	0.171	S5
MOF 1	ODZ	0.15	This work

SUPPORTING INFORMATION

Table S4. HOMO and LUMO Energies for the Selected Antibiotics Calculated by DFT B3LYP/6-31G*

Analytes	HOMO (ev)	LUMO (ev)
ODZ	-6.283	-3.268
THI	-6.206	-2.661
FFC	-6.620	-2.560
SDZ	-5.538	-2.260
CFX	-5.938	-2.186
PCL	-5.558	-1.777
CFD	-6.217	-1.467
SMZ	-6.467	-1.092
ACL	-6.001	-0.526

SUPPORTING INFORMATION

Table S5. Comparison of Detection Capacities of **1** toward Hg²⁺ with Other Reported MOF Materials

MOFs	Analyte	LOD (μM)	Ref.
[Co(NPDC)(bpee)]·DMF·2H ₂ O	Hg ²⁺	4.1	S6
[(CH ₃) ₂ NH ₂] ⁺ [Co(HCOO) ₃] _n	Hg ²⁺	0.783	S7
[Zn(tpbpc) ₂]·solvent	Hg ²⁺	0.32	S8
BA-Eu-MOF	Hg ²⁺	0.22	S9
MOF 1	Hg ²⁺	0.094	This work

n REFERENCES

- S1. Zhang, Q. F.; Geng, A. J.; Liu, Z. P.; Shi, Y.; Sun, D. Z. Synthesis, characterization, crystal structure and fluorescence property of tetramethyl 5,5-(terephthaloylbis(azanediyl))-diisophthalate. *J. Chem. Crystallogr.* **2012**, 42, 1124-1128.
- S2. Dong, B. X.; Pan, Y. M.; Liu, W. L.; Teng, Y. L. An ultrastable luminescent metal-organic framework for selective sensing of nitroaromatic compounds and nitroimidazole-based drug molecules. *Cryst. Growth Des.* **2018**, 18, 431-440.
- S3. Li, B.; Jiang, Y. Y.; Sun, Y. Y.; Wang, Y. J.; Han, M. L.; Wu, Y. P.; Ma, L. F.; Li, D. S. The highly selective detecting of antibiotics and support of noble metal catalysts by a multifunctional Eu-MOF. *Dalton Trans.* **2020**, 49, 14854-14862.
- S4. Li, J. M.; Huo, R.; Li, X.; Sun, H. L. Lanthanide-organic frameworks constructed from 2,7-naphthalenedisulfonate and 1*H*-Imidazo[4,5-*f*][1,10]-phenanthroline: synthesis, structure, and luminescence with near visible light excitation and magnetic properties. *Inorg. Chem.* **2019**, 58, 9855-9865.
- S5. Wei, J. H.; Yi, J. W.; Han, M. L.; Li, B.; Liu, S.; Wu, Y. P.; Ma, L. F.; Li, D. S. A new water-stable terbium(III)-organic framework as a chemosensor for inorganic ions, nitro-compounds and antibiotics in aqueous solutions. *Chem. Asian J.* **2019**, 14, 3694-3701.
- S6. Li, F.; Hong, Y. S.; Zuo, K. X.; Sun, Q.; Gao, E. Q. Highly selective fluorescent probe for Hg^{2+} and MnO_4^- by the two-fold interpenetrating metal-organic framework with nitro functionalized linkers. *J. Solid State Chem.* **2019**, 270, 509-515.
- S7. Thakur, N.; Pandey, M. D.; Pandey, R. Co(II)-catalyzed decarboxylation of itaconic acid engendering methacrylic acid and Co(II)-MOFs for structure regulated fluorescent detection of cations. *J. Solid State Chem.* **2019**, 280, 120987.
- S8. Xiao, J. N.; Liu, J. J.; Gao, X. C.; Ji, G. F.; Wang, D. B.; Liu, Z. L. A multi-chemosensor based on Zn-MOF: ratio-dependent color transition detection of Hg^{2+} and highly sensitive sensor of $\text{Cr}^{(VI)}$. *Sensor. Actuat. B-Chem.* **2018**, 269, 164-172.
- S9. Wang, H.; Wang, X. L.; Liang, M. S.; Chen, G.; Kong, R. M.; Xia, L.; Qu, F. L. A boric acid-functionalized lanthanide metal-organic framework as a fluorescence “turn-on” probe for selective monitoring of Hg^{2+} and CH_3Hg^+ . *Anal. Chem.* **2020**, 92, 3366-3372.